Modelling and Simulation
Practical Assignment I: The Chirikov map

Rick van Veen (s1883933)* Laura Baakman (s1869140)*

September 28, 2015

1. Introduction

This paper discusses the Chirikov map, since we are only interested in the non-integer part we use the following modified map:

(1a)
$$p_{n+1} = p_n + \frac{K \sin(2\pi x_n)}{2\pi} \mod 1$$
(1b)
$$x_{n+1} = x_n + p_{n+1} \mod 1,$$

where the non-linearity parameter $K \in \mathbb{R}$. The modulo operator ensures that $x_n, p_n \in [0, 1]$. In this paper we discuss the influence of the different parameters on the orbits in the map.

2. Experiments

We perform two different experiments with the Chirikov map, which is defined in equation (1). In section 2.1 we fix the value of the non-linearity parameter and explore the influences of different values for p_0 and x_0. In section 2.2 we discuss the influence of the non-linearity parameter K. Plotting various Chirikov maps with randomly chosen initial conditions for $K = 1$ results in decorative images, such as the one presented in figure 1.

2.1. Fixed K

We have fixed the value of K to 1, essentially removing the parameter from the equation. By choosing different initial values we can generate three different types of orbits: zero-, one- and two-dimensional. The three orbit types are discussed in respectively section 2.1.1, 2.1.2 and 2.1.3.

*These authors contributed equally ot this work.

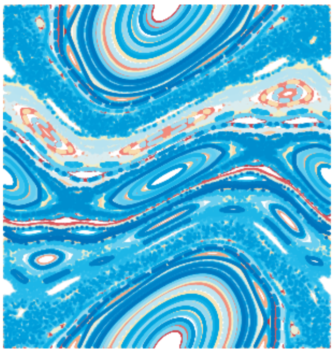

Figure 1: *Phase-space diagram, p_n as a function of x_n, of 500 randomly initialized orbits of the Chirikov map for $K = 1$, with $0 \leq n \leq 1000$, and x_0 and p_0 in the unit square.*

2.1.1. Discrete Points

Zero-dimensional orbits consist of a finite number of points, which are found in the centres of the islands in figure 1 [3]. We first discuss a specific initialization that results in such an orbit, before moving to the general case.

We have generated a zero-dimensional Chirikov map by choosing $x_0 = p_0 = 0.5$. Using these values $p_1 = p_0$ since the second term of (1a) becomes zero. This results in

$$x_1 = (x_0 + p_1) \mod 1 = 0.$$

The next steps of the map, for $n > 0$, are easily derived since p_{n+1} will not change due to the fact that both 0 and 0.5 as input to (1a) result in the second term becoming zero.

With the initialization $\{x_0, p_0\} = \{0.5, 0.5\}$, $x_n \in \{0, 0.5\}$ for $n \geq 0$. To illustrate x_2 is $0.5 + 0 = 0.5$ which is equal to x_1. We have now shown that p_n is constant for $n \geq 1$ and that x_n jumps between 0 and 0.5, which is illustrated in figure 3d and figure 3g. This conclusion also explains the phase space diagram, figure 3a, and the plot in figure 3j.

Furthermore we have shown that these points are visited in a fixed order.

From this specific initialization we can derive the following constraints for p_0 and x_0; x_0 should be chosen in such a way that the sine in equation (1a) becomes 0, i.e. $x_0 \in \{0,\ 0.5,\ 1\}$. Due to the constraint on x_0,

$$p_{n+1} = (p_n \mod 1)\,,$$

which is equal to p_n, unless $p_n = 1$. Consequently

$$x_{n+1} = (x_n + p_n \mod 1)\,,$$

unless $p_1 = 1$. Formally, one should choose p_0 in such a way that:

$$([x_0 + (p_0 \mod 1)] \mod 1) \in \{0, 0.5, 1\}\,.$$

2.1.2. Closed curves

One-dimensional orbits are represented in the phase-space diagram in figure 1 as the closed curves around the islands formed by the zero-dimensional orbits.

We have determined empirically that $\{x_0\,, p_0\} = 1.58\mathrm{e}^{-1}, 9.71\mathrm{e}^{-1}$ results in closed curves. Figure 3b shows p_n as a function of x_n, figure 3e and 3h show the progression of respectively p and x.

Considering these figures we see that the progression of both p and x happens according to a fixed pattern with a seemingly periodic shift. Examining figure 3k we see that x, the orange dashed line, slowly moves from one extreme to the other, which is reflected in figure 3h. Considering p in figure 3k, the solid blue line, we find that its value moves between approximately 0.2 and 0.8, and then oscillates around that value before going back to the other value. This is represented in figure 3e by the high density areas in the lower left and upper right corners.

We can conclude that the points of figure 3b are visited in a fixed order. Colloquially one could say that the map starts by generating a low density version of figure 3b, see figure 2, which is then filled in by iterating over the figure

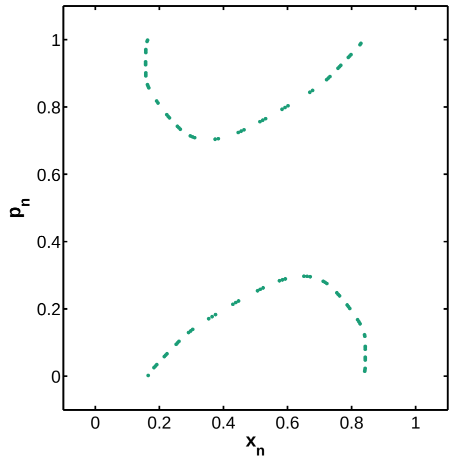

Figure 2: $p_n = 1.58\mathrm{e}^{-1}$ *as a function of* $x_n = 9.71\mathrm{e}^{-1}$, *for* $n = 100$.

multiple times. Due to the small shift, the area of the closed curve is filled in after a large number of iterations.

2.1.3. Two-Dimensional Orbits

Two-dimensional orbits fill entire areas by jumping around chaotically. The empirically determined values $\{x_0\,, p_0\} = 1.27\mathrm{e}^{-1},\ 9.13\mathrm{e}^{-1}$ result in an orbit that fills the two-dimensional areas in figure 3c.

Comparing figure 3e with figure 3f we see the same general pattern, however figure 3f shows more chaotic behaviour. We observe the same behaviour for x when contrasting figure 3h with figure 3i. This is supported by comparing figure 3k with figure 3l, where we find that the blue and orange lines have approximately the same trajectory, however the lines in figure 3l change more and with a varying value every period.

Since the map with orbits is essentially the same as the map with the closed curves the single points we can conclude that the points in the 2-dimensional map are also visited in a fixed order.

As the values of p and x vary more, plotting p as a function of x results in an area around the curves that we saw in figure 3b.

2.2. Variable K

The parameter K defines how hard the system is driven, that is why for $K = 0$ we would expect to

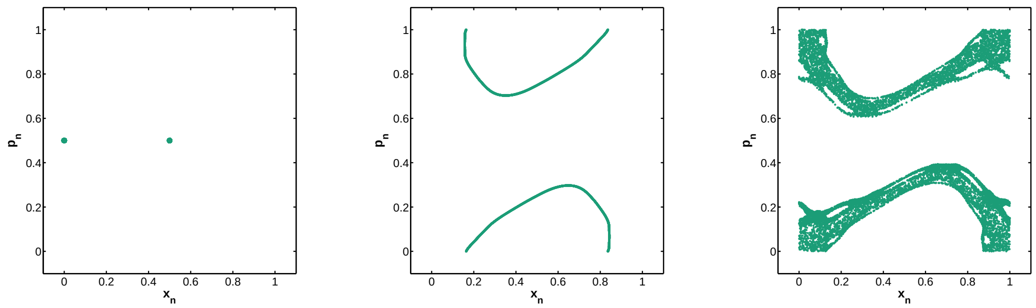

(a) $x_0 = 5.00\text{e}^{-1}$, $p_0 = 5.00\text{e}^{-1}$ **(b)** $x_0 = 1.58\text{e}^{-1}$, $p_0 = 9.71\text{e}^{-1}$ **(c)** $x_0 = 1.27\text{e}^{-1}$, $p_0 = 9.13\text{e}^{-1}$

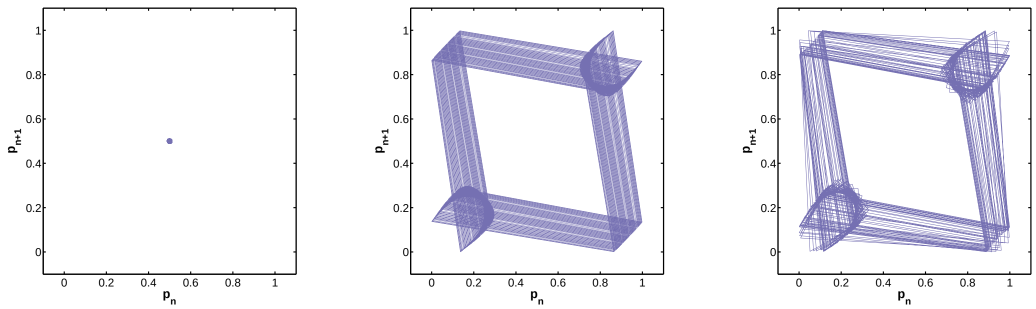

(d) *Progression of p in (a)* **(e)** *Progression of p in (b)* **(f)** *Progression of p in (c)*

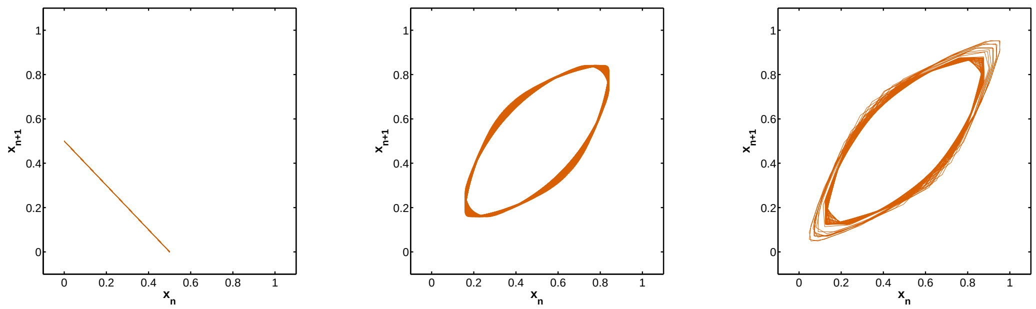

(g) *Progression of x in (a)* **(h)** *Progression of x in (b)* **(i)** *Progression of x in (c)*

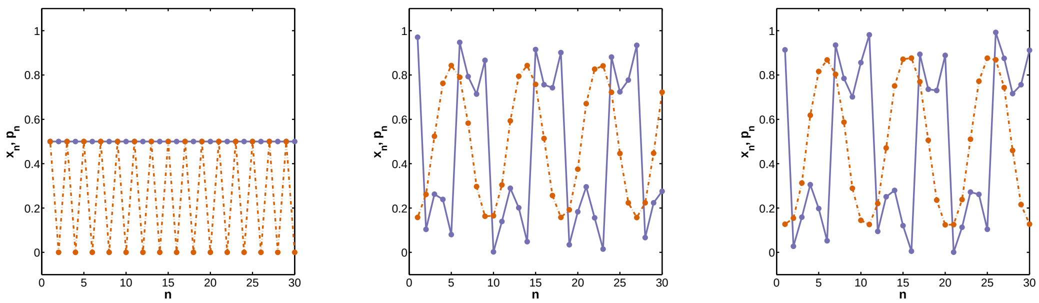

(j) $x(n)$ *and* $p(n)$ **(k)** $x(n)$ *and* $p(n)$ **(l)** $x(n)$ *and* $p(n)$

Figure 3: *Each column corresponds to one set of initial values* $\{x_0, p_0\}$. *The first row shows* x_n *versus* p_n *for* $n \in \left[0,\ 1.00\text{e}^{4}\right]$. *The second and third row depict respectively the progression of* p *and* x, *for* $0 \leq n \leq 500$. *The last row shows* x *and* p *as a function of* n. *The colours in last row of plots match those used in the second and third row.*

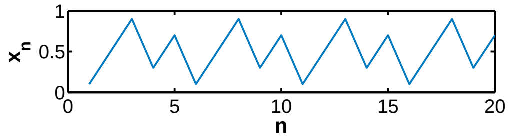

(a) $x_0 = 0.1$

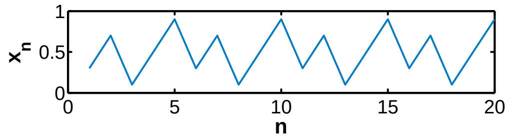

(b) $x_0 = 0.3$

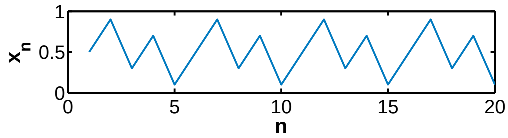

(c) $x_0 = 0.5$

Figure 4: *x_n as a function of n, for $p_0 = 0.4$,$K = 0$ and varying x_0.*

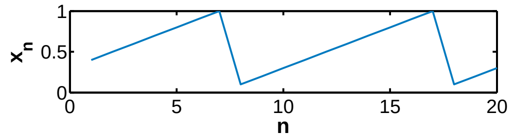

(a) $p_0 = 0.1$

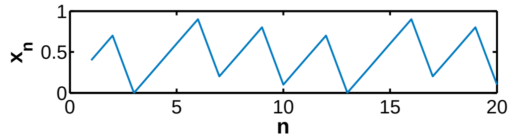

(b) $p_0 = 0.3$

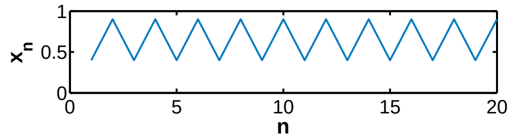

(c) $p_0 = 0.5$

Figure 5: *x_n as a function of n, for $x_0 = 0.4$, $K = 0$ and varying p_0.*

have no perturbations. The trival case, $K = 0$, is discussed in section 2.2.1.

As the value of K increases we expect that the chaotic regions grow and eventually start to dominate the phase space [1]. The effect of varying values of K is discussed in section 2.2.2.

Finally section 2.2.3 discusses KAM orbits in the context of the Chirikov map.

2.2.1. Trivial Case

If we choose $K = 0$ equation (1) becomes:

(2a)

$$p_{n+1} = p_n \mod 1,$$

(2b)

$$x_{n+1} = x_n + p_{n+1} \mod 1.$$

Consequently the values of p_n are constant for $n > 0$, since if $p_0 = 1$, then p_1 becomes zero as a consequence of the modulo operator in (2a). This effect is illustrated by the horizontal lines in figure 6a. Additionally without the modulo in (2b), x_n would increase linearly, due to this operator however x_n becomes periodic.

Figure 4 shows x_0 as a function of n for a fixed value of p_0, if we compare the different plots in this figure we observe that changing x_0 and fixing p_0 only influences the phase of x_n, and not the period.

Fixing x_0 and varying p_0 results in figure 5, these plots show that p_0 influences the periodicity of the map, that is increasing p_0, increases the frequency of x_n.

2.2.2. Non-Trivial Case

Figure 6 shows the influence of variable K. As noted before K determines the drive of the system resulting in more chaotic behaviour with a higher K. The images in figure 6 were created by plotting 100 Chirikov maps with randomly chosen values for x_0 and p_0. The colour for each map was determined by its initialisation. The mapping from the colours to the initial values are shown in figure 6i. Due to this mapping of colours we can see that up until $K = 1$ the colours stay in the same order, as opposed to $K = 2$ to $K = 4$ were this order is completely gone.

We consider a phase space to be more chaotic when there are more or bigger filled areas in the images. As can be expected from the discussion in our previous section the map created with $K = 0$ shows only horizontal lines, with fits with the constant p_n. Interesting is the difference in line types i.e. there are filled and dotted lines, indicating different periods for x_n. Note that the *resolution* of the map is important when looking at these maps as an illustration. I.e.

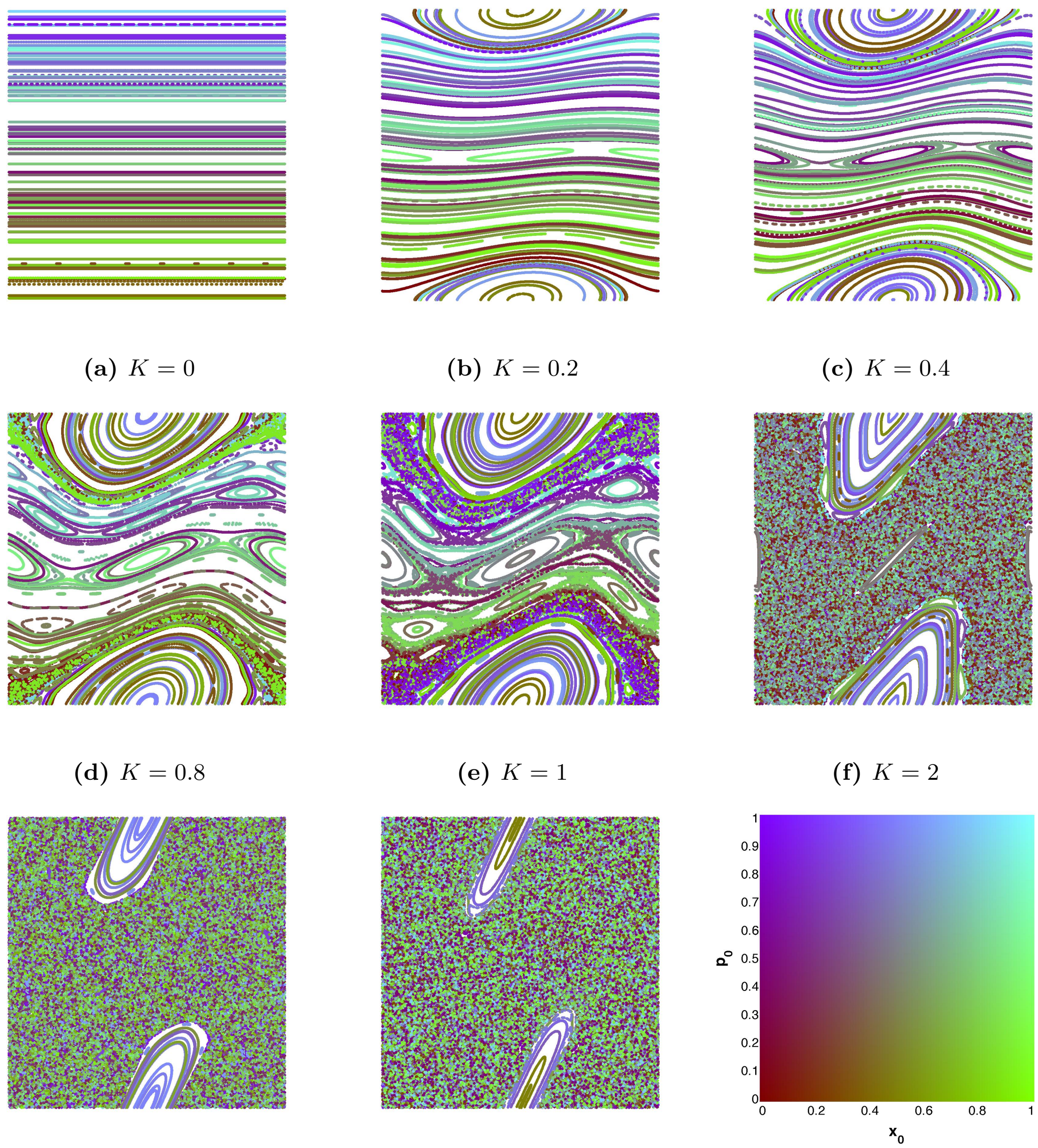

(a) $K = 0$ **(b)** $K = 0.2$ **(c)** $K = 0.4$

(d) $K = 0.8$ **(e)** $K = 1$ **(f)** $K = 2$

(g) $K = 3$ **(h)** $K = 4$ **(i)** *Color map*

Figure 6: *p_n (y-axis) as a function of x_n (x-axis) for p_0 and x_0 in the unit square, $0 \leq n \leq 1000$ for different values of K. Each plot shows 100 Chirikov maps with random intiaisations of x_0 and p_0. (i) shows the colourmap for (a) through (h).*

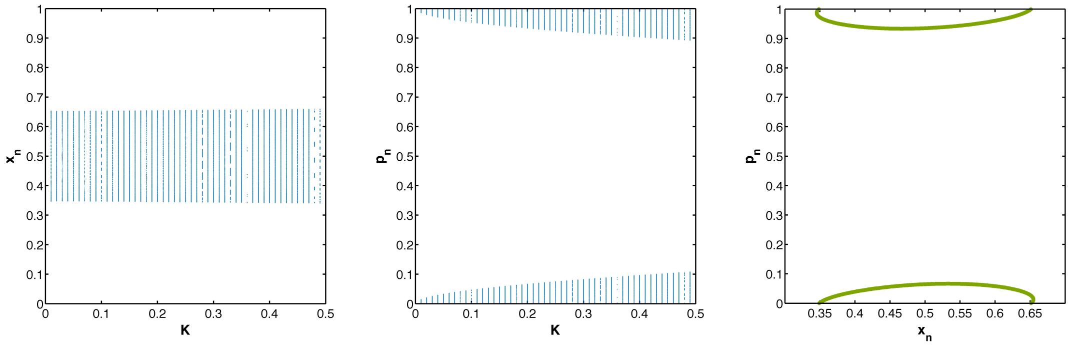

(a) $x_0 = 6.52\mathrm{e}^{-1}$

(b) $p_0 = 2.23\mathrm{e}^{-3}$

(c) *The orbit* $(K = 0.2)$

Figure 7: *Bifurcation plots and corresponding orbit for* $x_0 = 6.52\mathrm{e}^{-1}$ *and* $p_0 = 2.23\mathrm{e}^{-3}$ *to illustrate the period doubling like effect.*

some dashed line may appear to be solid line because of the choice of point size and scale of the illustration. Also the maps shown in this paper were created using a finite number of steps. It might be the case that some high frequency periodic behaviour converges to one period when more steps are calculated.

At $K = 0.2$ we see that some of the horizontal lines from figure 6a are replaced by closed curves in the upper and lower part of the image, see figure 6b. Because the colours in the image map to initial values we see that the curves that appear in the upper and lower part have approximately the same initial values. This resembles a kind of period doubling. Figure 7 shows this period doubling like behaviour in a bifurcation diagram, together with the corresponding orbit which resembles the one we described.

In Figure 6d we can see that chaos increases ($K = 0.8$), as some regions are already starting to be filled in by two-dimensional orbits, they are especially noticeable in the corners of the plot.

Finally in the images shown in figure 6f - 6h we see that the chaotic orbits start to completely dominate the image. With in the last two images (figure 6g and 6h) only a few stable initialisations left.

2.2.3. KAM-orbits

Kenzel et al. define Kolmogorov-Arnold-Moser-orbits as one-dimensional orbits that traverse the entire phase-state diagram horizontally. These KAM orbits are represented by the solid lines in figure 6. Looking closely at figure 6a we observe that not all orbits are KAM-orbits, since some of the lines are clearly dashed. Note that here the *resolution problem*, as discussed in the previous section, also has to be considered. An interesting property of the KAM-orbits is that it can be shown that chaotic orbits cannot cross the one-dimensional orbits [3]. Consequently they restrict the extent of the chaos of the two-dimensional orbits.

Greene observed that for small values of K there are many KAM orbits that encircle the islands horizontally, see figure 6a, 6b and 6c. These KAM orbits divide the space into several compartments which may contain chaotic orbits. For larger values of K there are fewer KAM orbits and individual chaotic orbits occur a greater are of the phase space. Finally at some critical value of K, called K_c, the last KAM orbit disappears, this effect can be observed in figure 6e.

It has been found that for $K < K_c = 0.971635\ldots$, one-dimensional-orbits exist that traverse the entire phase-state diagram horizontally [3]. If we plot the phase-state diagram for a value of K that is slightly smaller than K_c, figure 8a, and for $K = K_c$, figure 8b, we observe that the single KAM-orbit in figure 8a has disappeared in figure 8b.

3. Conclusion

In our discussion of the Chirikov map we have seen some similarities with the logistic map.

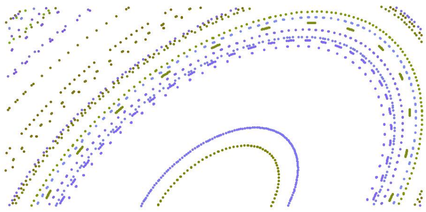

(a) $K = 0.970000$

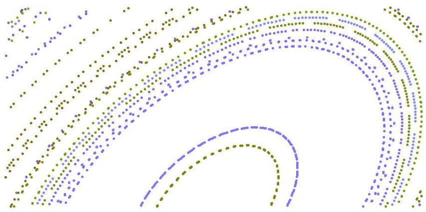

(b) $K = K_c$

Figure 8: *p_n as a function of x_n for $0.4 \leq x_n \leq 0.6$, $0 \leq p_n \leq 0.15$ and $0 \leq n \leq 250$. (a) show the phase-state diagram for $K = 0.970000$ and (b) for $K + K_c$. The 200 initial values for p and x where chosen randomly, but were identical for both values of K.*

Both maps are non-linear i.e. they produce output that is not necessary proportional to the input.

Both maps are driven by a variable which determines the amount of chaos in the system. Meaning that setting this non-linearity parameter will remove any and all chaotic behaviour, and choosing a low value for this parameter limits the chaos. This effect is illustrated for the Chirikov map in figure 6 where for low K values the x_n and p_n values stay approximately in the same area, when K is small.

An important difference is that the Chirikov map produces two dimensional output, which also depend on each other, see (1), whereas the logistic map only produces a one-dimensional map.

For the logistic map it can be shown that there is period doubling, although the Chirikov map exhibits behaviour that is reminiscent of period doubling, it does not have period doubling.

References

[1] Conor Finn. "Chaotic Control Theory Applied to the Chirikov Standard Map". Bachelor Thesis. Warwick University, 2012.

[2] John M Greene. "A method for determining a stochastic transition". In: *Journal of Mathematical Physics* 20.6 (1979), pp. 1183–1201.

[3] Wolfgang Kenzel et al. *Physics by computer*. Springer-Verlag New York, Inc., 1997.